VTRC
Virginia Transportation Research Council

Investigation of Properties of High-Performance Fiber-Reinforced Concrete: Very Early Strength, Toughness, Permeability, and Fiber Distribution

http://www.virginiadot.org/vtrc/main/online_reports/pdf/17-r3.pdf

EVELINA KHAKIMOVA, EIT
Graduate Research Assistant

CELIK OZYILDIRIM, Ph.D., P.E.
Principal Research Scientist

Final Report VTRC 17-R3

VIRGINIA TRANSPORTATION RESEARCH COUNCIL
530 Edgemont Road, Charlottesville, VA 22903-2454
www.VTRC.net

Standard Title Page - Report on Federally Funded Project

1. Report No.: FHWA/VTRC 17-R3	2. Government Accession No.:	3. Recipient's Catalog No.:
4. Title and Subtitle: Investigation of Properties of High-Performance Fiber-Reinforced Concrete: Very Early Strength, Toughness, Permeability, and Fiber Distribution		5. Report Date: January 2017 6. Performing Organization Code:
7. Author(s): Evelina Khakimova, EIT, and Celik Ozyildirim, Ph.D., P.E.		8. Performing Organization Report No.: VTRC 17-R3
9. Performing Organization and Address: Virginia Transportation Research Council 530 Edgemont Road Charlottesville, VA 22903		10. Work Unit No. (TRAIS): 11. Contract or Grant No.: 106439
12. Sponsoring Agencies' Name and Address: Virginia Department of Transportation 1401 E. Broad Street Richmond, VA 23219 Federal Highway Administration 400 North 8th Street, Room 750 Richmond, VA 23219-4825		13. Type of Report and Period Covered: Final 14. Sponsoring Agency Code:
15. Supplementary Notes:		

16. Abstract:

Concrete cracking, high permeability, and leaking joints allow for intrusion of harmful solutions, resulting in concrete deterioration and corrosion of reinforcement in structures. The development of durable, high-performance concretes with limited cracking is a potential solution for extending the service life of concrete structures. Further, the use of very early strength durable materials will facilitate rapid and effective repairs, reduce traffic interruptions, and decrease long-term maintenance work.

The purpose of this study was to develop low-permeability durable materials that could achieve a very early compressive strength of 3,000 psi within 10 hours. Within the scope of this work, various proportions of silica fume and fly ash and steel and polypropylene fibers were used to evaluate crack control and post-cracking performance. Other characteristics including toughness, residual strength, water permeability of cracked concrete, and fiber distribution were also examined.

The study showed that very early strength durable concretes can be achieved with proper attention to mixture components (amounts of portland cement and accelerating admixtures), proportions (water–cementitious materials ratio), and fresh concrete and curing temperatures. Fiber-reinforced concretes with steel fibers had considerably higher toughness and residual strength compared to concretes with polypropylene fibers. Permeability work showed that minor increases in crack width caused large increases in infiltration of solutions. Further, the addition of fibers can facilitate crack width control. An investigation of fiber distribution showed preferential alignment and some clumping of fibers in the specimens and highlighted the need for appropriate specimen size selection, sufficient mixing time, and proper sequencing of concrete ingredients into the mixer for a uniform random fiber distribution.

The results indicated that very early strength and durable fiber-reinforced concrete materials can be developed to improve the condition of existing and new structures and facilitate rapid, effective repairs and construction. The addition of fibers enables cracking control. Optimization of mixtures for strength and durability at different ages for specific applications is recommended.

17 Key Words: fiber reinforced concrete, very early strength, steel fibers, polypropylene fibers, toughness, residual strength, permeability of cracked concrete, fiber distribution		18. Distribution Statement: No restrictions. This document is available to the public through NTIS, Springfield, VA 22161.	
19. Security Classif. (of this report): Unclassified	20. Security Classif. (of this page): Unclassified	21. No. of Pages: 31	22. Price:

Form DOT F 1700.7 (8-72) Reproduction of completed page authorized

FINAL REPORT

INVESTIGATION OF PROPERTIES OF HIGH-PERFORMANCE FIBER-REINFORCED CONCRETE: VERY EARLY STRENGTH, TOUGHNESS, PERMEABILITY, AND FIBER DISTRIBUTION

Evelina Khakimova, EIT
Graduate Research Assistant

Celik Ozyildirim, Ph.D., P.E.
Principal Research Scientist

In Cooperation with the U.S. Department of Transportation
Federal Highway Administration

Virginia Transportation Research Council
(A partnership of the Virginia Department of Transportation
and the University of Virginia since 1948)

Charlottesville, Virginia

January 2017
VTRC 17-R3

DISCLAIMER

The contents of this report reflect the views of the authors, who are responsible for the facts and the accuracy of the data presented herein. The contents do not necessarily reflect the official views or policies of the Virginia Department of Transportation, the Commonwealth Transportation Board, or the Federal Highway Administration. This report does not constitute a standard, specification, or regulation. Any inclusion of manufacturer names, trade names, or trademarks is for identification purposes only and is not to be considered an endorsement.

ABSTRACT

Concrete cracking, high permeability, and leaking joints allow for intrusion of harmful solutions, resulting in concrete deterioration and corrosion of reinforcement in structures. The development of durable, high-performance concretes with limited cracking is a potential solution for extending the service life of concrete structures. Further, the use of very early strength durable materials will facilitate rapid and effective repairs, reduce traffic interruptions, and decrease long-term maintenance work.

The purpose of this study was to develop low-permeability durable materials that could achieve a very early compressive strength of 3,000 psi within 10 hours. Within the scope of this work, various proportions of silica fume and fly ash and steel and polypropylene fibers were used to evaluate crack control and post-cracking performance. Other characteristics including toughness, residual strength, water permeability of cracked concrete, and fiber distribution were also examined.

The study showed that very early strength durable concretes can be achieved with proper attention to mixture components (amounts of portland cement and accelerating admixtures), proportions (water–cementitious materials ratio), and fresh concrete and curing temperatures. Fiber-reinforced concretes with steel fibers had considerably higher toughness and residual strength compared to concretes with polypropylene fibers. Permeability work showed that minor increases in crack width caused large increases in infiltration of solutions. Further, the addition of fibers can facilitate crack width control. An investigation of fiber distribution showed preferential alignment and some clumping of fibers in the specimens and highlighted the need for appropriate specimen size selection, sufficient mixing time, and proper sequencing of concrete ingredients into the mixer for a uniform random fiber distribution.

The results indicated that very early strength and durable fiber-reinforced concrete materials can be developed to improve the condition of existing and new structures and facilitate rapid, effective repairs and construction. The addition of fibers enables cracking control. Optimization of mixtures for strength and durability at different ages for specific applications is recommended.

FINAL REPORT

INVESTIGATION OF PROPERTIES OF HIGH-PERFORMANCE FIBER-REINFORCED CONCRETE: VERY EARLY STRENGTH, TOUGHNESS, PERMEABILITY, AND FIBER DISTRIBUTION

Evelina Khakimova, EIT
Graduate Research Assistant

Celik Ozyildirim, Ph.D., P.E.
Principal Research Scientist

INTRODUCTION

New construction and rehabilitation of existing structures require high-performance durable materials that facilitate extension of the service life of concrete structures with minimal maintenance. The National Bridge Inventory (NBI) estimated that in 2014 about 10% of bridge structures in the United States were considered structurally deficient. About 6.2% of the Virginia Department of Transportation's (VDOT) National Bridge Inventory (NBI) and non-NBI structures were considered structurally deficient at the end of Fiscal Year 2015 (VDOT, 2015). Although the percentage of structurally deficient structures decreased during Fiscal Year 2015, there is still a large number of structures requiring immediate rehabilitation. According to the latest 2015 NBI database, about 50% of highway bridges in Virginia used concrete as the superstructure material (NBI, 2015). Therefore, the use of durable high-performance concretes (HPCs) to facilitate an extension of the service life of transportation structures is essential.

The durability of concrete greatly depends on its strength, resistance to cracking, and permeability (Shah and Wang, 1997). Volumetric changes because of moisture and temperature, chemical reactions, or excessive loading are often the primary cause of concrete cracking. The intrusion of water and harmful solutions through these cracks and highly permeable concrete results in corrosion of the steel reinforcement and deterioration of the concrete through sulfate attacks, alkali-silica reactions, and freeze-thaw damage. Hence, the use of durable concrete mixtures with a high resistance to cracking and a low permeability is expected to increase the service life of structures.

The addition of supplementary cementitious materials (SCMs) has been shown to improve concrete durability and reduce its permeability. Further, the addition of fibers helps limit concrete deterioration by minimizing crack occurrence and by producing tighter cracks. As a consequence, cracked concretes reinforced with fibers have lower permeability than unreinforced cracked concretes (Rapoport et al., 2001). Large volumes of steel and polypropylene fibers (0.5% to 2.0% by volume) are expected to improve greatly the post-cracking performance of the concrete and increase its durability, residual strengths, and

toughness (American Concrete Institute [ACI], 2009). In addition to the use of durable materials, the repair time is of great importance. Rapid concrete placement and repairs would allow for accelerated construction and reductions in traffic interruptions and commuter costs (Sprinkel, 2006). Therefore, high-performance, early strength, fiber-reinforced concrete (FRC) mixtures comprise a promising technology that may satisfy the requirements for rapid construction and durability.

BACKGROUND

The Federal Highway Administration started the implementation of HPC in 1991. By 2005, the majority of the states had specifications for low-permeability HPCs (Vanikar and Triandafilou, 2005). HPC is often defined as concrete with enhanced short-term and long-term properties. High strength, high toughness, low permeability, long-term durability, good workability, and other parameters often represent HPCs (Nawy, 2001). In the transportation industry, early HPC developments were commonly described as concretes with low permeability and high strength (Ozyildirim, 1993). The use of SCMs and a low water–cementitious materials ratio (w/cm) enabled the reduction of concrete permeability and increased ultimate strength.

The development of very early strength (VES) concrete and its performance have been investigated by a number of researchers, and they remain topics of continued study, as the properties are constantly being enhanced. The VES properties depend on cement type, amount of paste, w/cm, fresh concrete and curing temperatures, and addition of SCMs and chemical admixtures (Kosmatka and Wilson, 2011). There are no minimum strength criteria for the VES concrete mixtures described in available standards or research work. According to Parker and Shoemaker (1991) in their study of concrete pavement patching materials, a compressive strength of 2,000 psi is sufficient to open the patches to traffic. Hence, concretes that can achieve compressive strengths of 2,000 psi and higher in a matter of several hours could be considered VES concretes.

Punurai et al. (2007) conducted a study on VES concrete using high amounts of Type I cement, accelerating admixture, and fresh concrete temperatures above 82 °F to achieve the required early strength. The VES concretes reached more than 2,250 psi in compressive strength and more than 350 psi in flexural strength in about 6.5 hours. Further, VDOT has successfully used Rapid Set cement concrete mixtures with latex in concrete overlays to obtain VES strength and low-permeability mixtures. Latex-modified concrete (LMC) with very early strength (LMC-VE) can achieve a compressive strength of more than 2,500 psi in 3 hours, which allows for rapid repairs and early lane opening to traffic. Other benefits of LMC-VE include low permeability and very low shrinkage. Hence, the LMC-VE overlay system effectively protects bridge decks at “a minimum of inconvenience to the traveling public” (Sprinkel, 2006).

Some of the main drawbacks of VES concretes are increased thermal and autogenous shrinkage and an increased elastic modulus. The use of high early strength cements, high fresh concrete temperatures, high cement amounts, and low w/cms causes greater heat generation at

early ages (Mehta and Burrows, 2001). Hence, there is a high risk of cracking, potentially leading to a decrease in concrete durability. The long-term strength is also negatively affected by the high temperatures at early ages (Klieger, 1958; Nawy, 2001). The increase in fresh concrete temperature also causes decreased slump and increased water demand (Klieger, 1958). Further, the cost of VES concretes is usually high compared to that of normal strength concretes because of the addition of accelerating admixtures and use of special cements and higher amounts of cementitious material. The durability characteristics of VES concretes could be improved through the addition of SCMs and fibers.

Class F fly ash (FA) generally constitutes from 15% to 25% of total cementitious material in concrete mixtures, and because of the spherical shape of the FA particle, it facilitates the reduction of water demand, increase in workability, and reduction of bleeding and segregation. FA increases concrete setting time because it replaces portland cement, causes pozzolanic reactions, and lowers heat of hydration. Silica fume (SF) is a very fine material and generally makes up from 5% to 10% of total cementitious material in concrete mixtures. Lower permeability and increased early-age strength could result from its use (Kosmatka and Wilson, 2011). However, it also increases water demand, especially in higher replacement rates, and decreases workability and air content. Further, SF is more expensive than FA.

The addition of various types of fibers for enhancement of concrete properties has been in practice since the 1960s (ACI, 2009). With the addition of fibers, concrete crack formation is more controlled, and concrete failure becomes less brittle with the ability to sustain further strains and stresses. Researchers at the Virginia Transportation Research Council (VTRC) have been studying properties of FRC for a number of years. Between 1993 and 1997, Ozyildirim et al. (1997) studied applications of FRC for use in the transportation industry. The study concluded that with increases in fiber content, the FRC impact resistance and toughness considerably improve, with the steel fibers performing better than the synthetic fibers. The optimal FRC mixtures were implemented in a series of Virginia bridge overlay projects. Visual surveys showed that FRC sections had tighter cracks than the control sections without fibers (Ozyildirim et al., 1997). Further, it has been shown that with crack widths less than 0.1 mm, steel fibers do not exhibit any corrosion (Granju and Balouch, 2005). When corrosion occurs with wider cracks, the corrosion product does not penetrate more than 1 mm into the concrete. Mangat et al. (1987) demonstrated that with crack widths less than 0.15 mm, corrosion does not occur in low carbon steel FRC.

Concrete permeability and fiber distribution greatly influence the performance and service life of concrete structural elements. Concrete permeability is one of the most important durability characteristics of concrete. Intrusion of harmful solutions through sound high-permeability concrete or through cracked concrete can deteriorate the material and lead to corrosion of reinforcing steel (Kosmatka and Wilson, 2011). A number of studies have been conducted to investigate the permeability of cracked concrete. Aldea et al. (1999) considered the effects of specimen thickness, average crack width, and material constituents. The results of the study indicated that crack widths less than 0.1 mm do not have an effect on the permeability of

concrete. A rapid permeability increase occurred for concrete with cracks wider than 0.1 mm. Further, ACI (2001) considers 0.1 mm a reasonable crack width for water-retaining structures.

The distribution of fibers in concrete mixtures can influence the performance of concrete. Potential clumping of fibers during mixing and internal and external vibrations of the FRC mixtures during placement can impact fiber distribution. The workability of concrete and placement techniques can influence fiber alignment and potentially lead to fiber settlement.

In concrete sections without fibers (because of fiber clumping), less energy is required to form and propagate cracks, and acting as defects, the fiber-free areas detrimentally affect the mechanical performance of FRCs (Akkaya et al., 2000a, 2000b, 2001). At the same time, because of random fiber distribution, only a certain amount of fibers are properly oriented and aligned to resist tensile and flexural stresses efficiently (Portland Cement Association, 1991). The relationship between the fiber distribution and orientation and the tensile and flexural strengths of ultra-high strength FRC was previously investigated (Kang and Kim, 2011, 2012; Kang et al., 2011). It was seen that the fiber distribution depends on the casting direction and, in turn, has a large effect on post-cracking performance. The longitudinal fiber alignment was beneficial to the post-cracking flexural and tensile capacities. Further, statistical spatial point pattern analysis can be used to examine the fiber distribution. Statistical functions can be used to quantify the tendency of fiber clumping (K-function) and describe the areas without fibers (F-function). Akkaya et al. (2001) studied spatial fiber distribution of polyvinyl alcohol fibers in cement and SF composite systems. The locations of the first several cracks were related to higher fiber clumping and higher statistical K-function values; whereas later cracks coincided with more of a random dispersion and lower K-function values. The first crack location also had lower values of the statistical F-function, meaning a higher number of areas without fibers. The statistical functions are further discussed in the Appendix.

PURPOSE AND SCOPE

The purpose of this study was to develop durable concrete mixtures with very early strength, low permeability, and resistance to cracking. The desired compressive strength was 3,000 psi within 10 hours. The mixtures included SCMs for durability and different types and volumes of fibers for crack resistance. The compressive and flexural strengths and drying shrinkage were determined. Other characteristics such as toughness, residual strength, water permeability of cracked concrete, and fiber distribution were also examined.

The study focused on concrete mixtures with two SCMs: fly ash and silica fume. Further, two types of fibers were used: steel and polypropylene. All mixing and testing were conducted at the VTRC concrete laboratory.

METHODS

Overview

The study was conducted in three stages.

- *Stage 1.* This stage focused on developing VES-FRC mixtures that could reach 3,000 psi compressive strength within 10 hours and was conducted in the laboratory. The investigation focused on mixture ingredients and admixture proportioning, fiber amounts, variation of w/cms, and variation of fresh concrete temperature and curing temperature. Preliminary plain concrete batches were prepared and tested for strength to attain the very early strengths. When satisfactory strengths were obtained, batches with fibers were prepared to determine characteristics other than compressive strength, such as flexural strength, toughness, residual strength, drying shrinkage, permeability of cracked specimens, and fiber distribution. Table 1 lists the test methods and specimen sizes used during this study. Two fiber types were considered: polypropylene (PP) and steel (S). Table 2 and Figure 1 show the characteristics of the fibers and their properties.

- *Stage 2.* This stage focused on testing the water permeability of cracked FRCs. Controlled crack widths of 0.1 to 0.5 mm (0.004 to 0.020 in) were formed in FRC and tested in accordance with the falling head permeability test (Virginia Test Method [VTM] 120).

- *Stage 3.* This stage investigated fiber distribution within the concrete mixtures and spatial fiber dispersion in the cross sections of the crack location.

Table 1. Test Methods for Concrete Properties

Property	Test Method	Specimen Size
Fresh Concrete Properties		
Air Content	ASTM C231	-
Slump	ASTM C143	-
Unit Weight	ASTM C138	-
Temperature	ASTM C1064	-
Hardened Concrete Properties		
Compressive Strength	ASTM C39	4 by 8 in cylinder
Elastic Modulus	ASTM C469	4 by 8 in cylinder
Flexural Strength	ASTM C1609	4 by 4 by 14 in beam
Shrinkage (Length Change)	ASTM C157	3 by 3 by 11 in beam
Splitting Tensile Strength (Crack Formation)	ASTM C496	6 by 2 in cylinder
Water Permeability (Falling Head)	Virginia Test Method 120	6 by 2 in cylinder
Maturity Test, Method 1	ASTM C1074	-
Maturity Test, Method 2	ASTM C918	-

Table 2. Characteristics of Fibers

Material	Polypropylene	Steel
Form	Monofilament, Crimped	Straight, Hooked Ends
Diameter (microns)	Data not available	900
Length (in)	2	2.36
Aspect Ratio	75	65
Specific Gravity	0.91	7.85
Tensile Strength (ksi)	80	335
Young's Modulus (ksi)	1,000	30,460
Wire Ductility	Data not available	6%

(a) **(b)**

Figure 1. Fiber Types: (a) Polypropylene; (b) Steel

Stage 1: Development of Very Early Strength Fiber-Reinforced Concretes (VES-FRCs)

The objective of this stage was to develop VES-FRC mixtures that could achieve a compressive strength of 3,000 psi within 10 hours. Figure 2 shows the breakdown of the VES-FRC mixture development process. First, batches without fibers were tested to achieve the very early strengths; second, mixtures with fibers were made.

The development of VES concretes mainly focused on the use of the following:

- increased cement contents
- reduced w/cms
- increased fresh concrete temperature
- higher amounts of accelerating admixtures to reduce concrete setting time and increase early strength gain
- insulated curing to retain heat and accelerate the strength development until the required strength was reached.

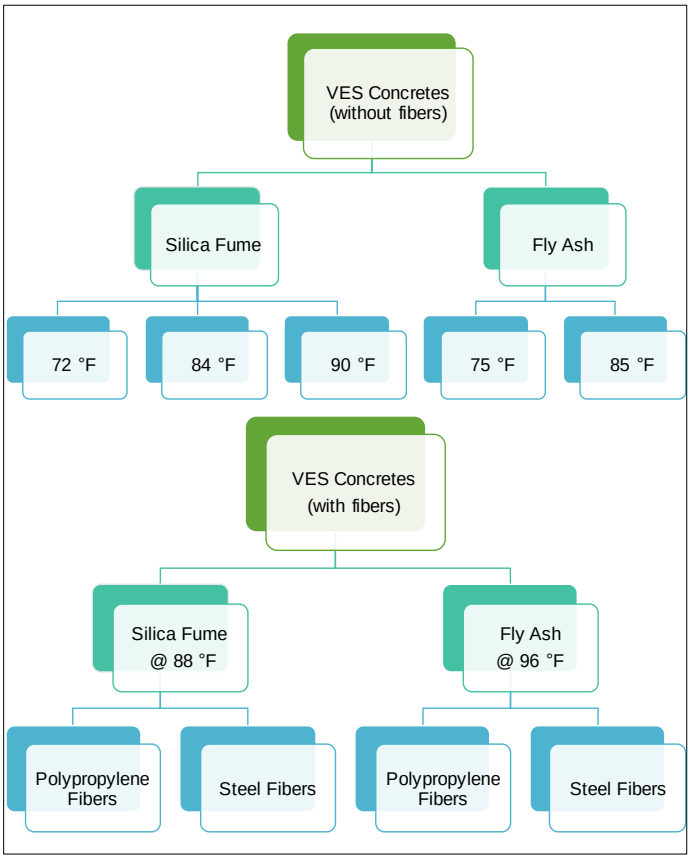

Figure 2. Development of VES-FRCs. PP = polypropylene fibers; S = steel fibers.

The VES w/ SF concretes without fibers were developed based on the ongoing research at VTRC and consultation with the industry. The mix design of VES w/ FA was adopted from the existing VDOT patching mixtures for pavement repairs, which require 2,000 psi compressive strength within 6 hours. Hence, the batches were tested for a strength requirement of 2,000 psi. The successful results led to the use of VES w/ FA patching mixtures in this study for a compressive strength of 3,000 psi within 10 hours.

The VES concretes were mixed and kept at different temperatures to determine the importance of fresh concrete and curing temperatures on the strength development. Exploratory VES w/ SF batches without fibers were made at three temperatures: 72 °F, 84 °F, and 90 °F. Two batches with VES w/ FA were made with fresh concrete temperatures at 75 °F and 85 °F. To obtain elevated fresh concrete temperatures, the mix water temperature was increased to 120 °F to 130 °F, whereas the aggregates and cementitious materials were kept at a room laboratory temperature of 73 °F.

After the VES concretes without fibers were mixed, two batches with PP or S fibers for each VES w/ SF and VES w/ FA mixture were made. Based on the fiber manufacturers' recommended dosages, 15 lb/yd^3 of PP fibers and 66 lb/yd^3 of S fibers were considered. The 15 lb/yd^{3}of PP fibers appeared to be the maximum amount that could be added without any major

mixing problems, such as fiber balling or clumping. The S fibers could be added at higher amounts, and 80 lb/yd^3 was tried to ensure improvements in the post-cracking behavior. The fiber dosages were within the manufacturer's recommended range and were limited by proper mixing and workability (upper limit) and desired properties (lower limit). Available natural sand fine aggregate and 0.5-in (No. 78) crushed coarse aggregate were used. Smaller size crushed coarse aggregate is recommended for use in high strength concrete (ACI, 2015). Ultimate strength is increased and bond strength improves because of the greater surface area of smaller aggregates (ACI, 2015). In addition, smaller aggregates facilitate workability, which reduces with the addition of fibers. The PP fibers were added at the beginning of mixing with coarse and fine aggregates to facilitate better fiber dispersion. There were no mixing issues for mixtures with S fibers. An air-entraining admixture and a high-range water-reducing admixture were used to achieve the specified air content and workability. Table 3 shows the VES-FRC laboratory mix designs. Two types of FRC having a different cementitious content, SCM, and w/cm were used to achieve the desired strength, permeability, and shrinkage.

Table 3. VES-FRCs Mix Designs

Component	VES-FRC w/ SF		VES-FRC w/ FA	
Ingredient (lb/yd^3)				
Cement Type I/II	750		750	
Silica Fume (6%)	50		-	
Class F Fly Ash (15%)	-		132	
Water	272		265	
Fine Aggregate	1437		1364	
Coarse Aggregate	1407		1407	
Total Cementitious Material	800		882	
w/cm	0.34		0.30	
PP (% by volume)	15 (1.0)	-	15 (1.0)	-
S (% by volume)	-	80 (0.6)	-	80 (0.6)
Admixtures (oz/cwt)				
Set Accelerating	24		24	
Hardening Accelerating	20		20	
Paste Content	0.32		0.33	
Mix Temperature (°F)	88		96	

w/cm = water–cementitious materials ratio; PP = polypropylene fibers; S = steel fibers.

For each batch the following specimens were made:

- Eight 4 in by 8 in cylinders were made to test compressive strength starting 6 hours after casting, then about every hour until a compressive strength of 3,000 psi was reached. Then the rest of the cylinders were tested at 1, 7, and 28 days.

- Three flexural beams were made to test at the time the 3,000 psi compressive strength was reached, and then later tested at 7 and 28 days. First-peak and peak flexural strengths, residual strengths, toughness, and the equivalent flexural strength ratio were determined in accordance with ASTM C1609 (ASTM International [ASTM], 2013).

- Two length change beams were made to determine the drying shrinkage development. The beams were subjected to moist curing for the first 7 days and then air dried for 4 months.

- Two 6 in by 12 in large cylinders for the cracked concrete water permeability testing were made; 2-in slices were cut and tested after 28 days.

Specimens were covered with plastic and insulating material and kept inside Styrofoam containers for the first 24 hours. Then the specimens were demolded and moved to the moisture room for 28 days. The relative humidity of the moisture room was above 95%, and the air temperature was about 73 ± 3 °F. Further, flexural beams and large cylinders were also kept inside the insulated containers (Figure 3). The temperatures of cylinders, the environment inside the containers, and the laboratory were recorded with the use of multiple thermocouples with a data logger.

Figure 3. VES-FRCs Specimens Curing for First 24 Hours

Stage 2: Permeability of Cracked FRC Specimens

For each FRC batch with S or PP fibers, 8 to 10 cylinders 6 in by 2 in were tested. Based on the literature review, the crack widths of 0.1 to 0.5 mm (0.004 to 0.020 in) were formed in accordance with the splitting tensile testing procedure (ASTM C496). The MTS Laser Extensometer LX500 was used to capture the horizontal displacement between the two reflective tapes in the center on one side of the specimen. In addition, the 9X transparent base magnifier with a 20 mm scale was used to observe the cracks with and without the applied load. The crack relaxation after unloading was determined. As expected, the crack width was not uniform along the crack length. Figure 4 shows the splitting tensile test setup and the magnifier. The comparison of crack widths under load between the recorded laser extensometer and observed magnifier values was performed.

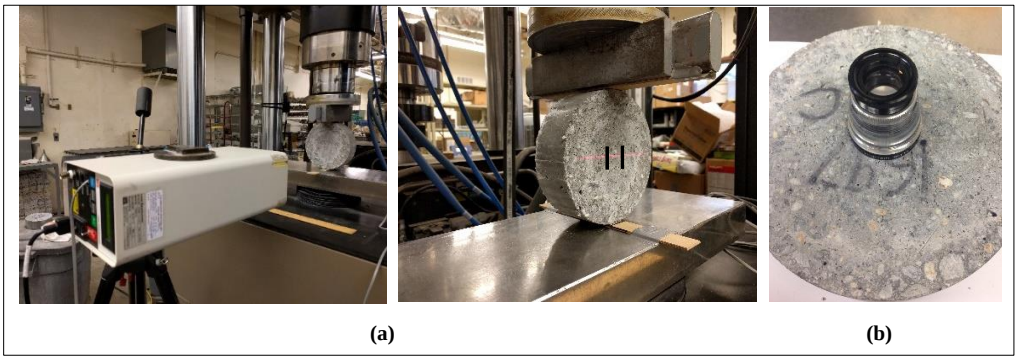

(a) (b)

Figure 4. (a) Splitting Tensile Test Setup; (b) Magnifier With Scale

The cracked specimens were saturated in accordance with ASTM C1202 for the permeability testing. Distilled water was used to saturate the cylinders. The specimens were vacuumed for 3 hours to remove trapped air, and then the distilled water was pumped into the container, with the pump running for 1 more hour. The specimens were then soaked for at least another 16 hours. The cracked concrete specimens were tested in accordance with VTM 120, Method for the Measurement of Permeability of Bituminous Paving Mixtures Using a Flexible Wall Permeameter (VDOT, 2005). VTM 120 is a falling head permeability test and is used to measure a coefficient of water permeability (CWP), i.e., the laminar water flow rate through the saturated sample. The time for the water to travel and the change in head level were recorded. Figure 5 shows the permeameter setup.

The water travel time for the 0.1, 0.2, 0.3, 0.4, and 0.5 mm cracks was approximately 30 minutes, 10 minutes, 2 minutes, 1.5 minutes, and 45 seconds, respectively. For the 0.1 mm cracks, the test procedure was stopped at 30 min and the water level was recorded at the corresponding height. In addition, several solid uncracked specimens were tested to make sure there was no water leakage between the specimens and the sealing tube. The water level did not move for several hours, confirming that no leakage was taking place, and the water flowed through the formed cracks.

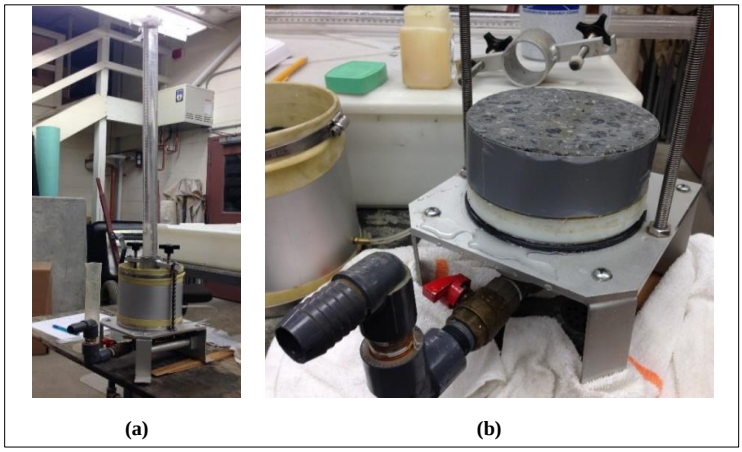

(a) (b)

Figure 5. Permeability Test: (a) Setup; (b) Specimen

The test was performed 3 times for each specimen, and the average CWP, *k*, was determined using Equation 1 (VDOT, 2005). In addition, the temperature of the water was measured and corrected to 68 °F.

$$k = \frac{a \cdot l}{A \cdot t} \cdot \ln\left(\frac{h_1}{h_2}\right) \qquad \text{[Eq. 1]}$$

where

k = coefficient of water permeability
a = standpipe area
A = average area of the specimen
l = average specimen thickness
t = average flow time
h_1 = initial hydraulic head
h_2 = final hydraulic head.

Stage 3: Fiber Distribution Analysis

This stage of this project was focused on fiber distribution. The flexural beams with PP and S fibers were sliced in the transverse (T) and horizontal (H) directions into 1-in-thick sections.

Figure 6 is a schematic of the ASTM C1609 test method with third-point flexural loading and the T and H cutting orientations for the two slicing methods: HTH and THTHT. Two beams with S fibers from each batch and one beam with PP fibers from each batch were used for the analysis. Each S fiber cross section was treated with a dark dye to create a high contrast between the S fibers and concrete. However, the same approach was not applicable for the cross sections with PP fibers; the individual fibers had to be marked with a permanent marker to highlight the fibers. Therefore, fewer specimens with PP fibers were analyzed because of the difficulty of observing the fibers.

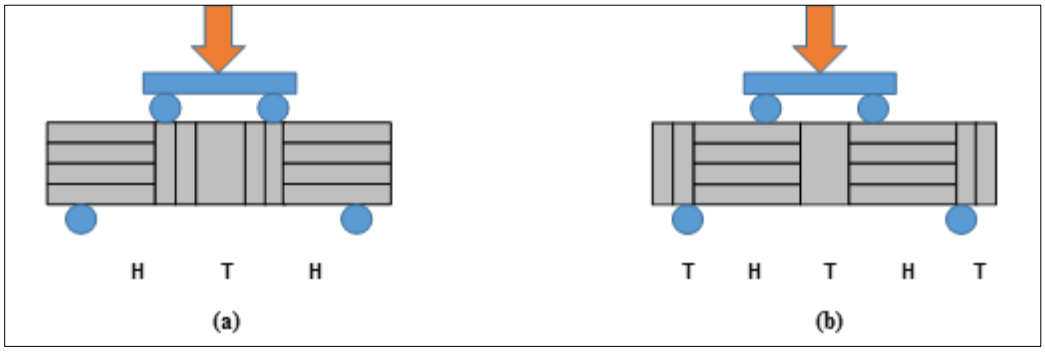

Figure 6. Schematic of Flexural Test Setup and Two Slicing Methods: (a) HTH, and (b) THTHT. H is a horizontal cut, and T is a transverse cut.

The digital images of the cross sections were taken and analyzed in MATLAB through image processing analysis. Step outputs of the MATLAB analysis code are displayed in Figure 7. Because of a random fiber orientation, the researchers decided to include only fibers oriented at the 45° angle or less in the fiber count.

Further, the spatial point pattern statistical analysis was performed to evaluate fiber dispersion. The point pattern analysis is used to determine the trend of the spatial dependence of the pattern. Figure 8 shows the representations of the clustered, regular (ordered), and random point patterns.

Fiber coordinates were determined from the image processing and analyzed through the statistical K-function and F-function (Diggle, 2003). The K-function represents the tendency of fiber clumping and measures the distance between fibers. The function considers a number of fibers within distance *s* of an arbitrary fiber in the cross section. Distance *s* was varied from 0 to one-half the width of the specimen. The F-function can be used to measure the empty spaces between the fibers. It determines the distribution of distances s from a random sample point in the cross section or from a generated grid point to its nearest fiber. Similarly, distance *s* was varied from zero to one-half the width of the specimen.

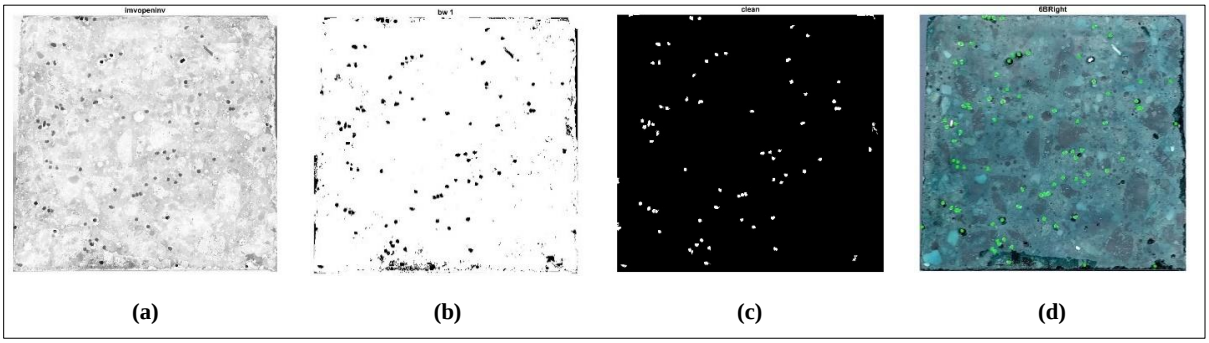

Figure 7. Image Analysis Process: (a) Inverse; (b) Binary; (c) Pixel Removal; (d) Final

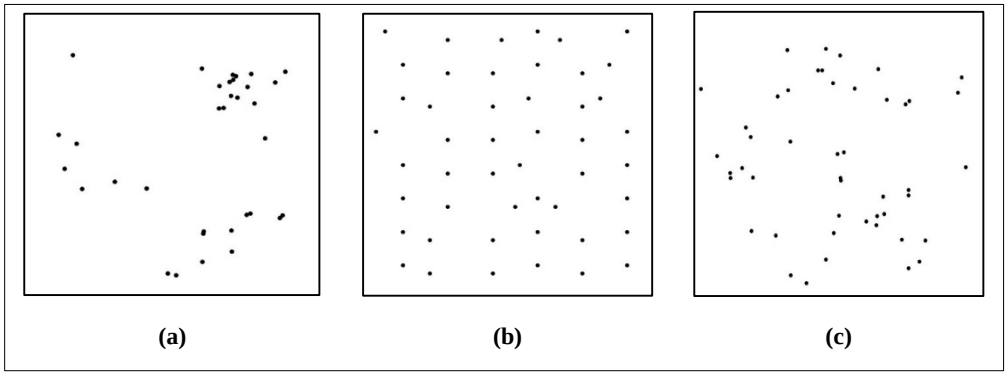

Figure 8. Point Patterns: (a) Clustered; (b) Regular; (c) Random. Adapted from Diggle (2003).

Random point pattern distribution can be described as a distribution under the complete spatial randomness (CSR) condition. The calculated K-function and F-function values are compared to the values obtained under the CSR condition: K-CSR and F-CSR, respectively. For the K-function, the clustering is observed for values greater than K-CSR, whereas the F-function values that drift below the F-CSR curve indicate a more aggregated (clustered) pattern, with more fiber-free areas. The function values that drift above the F-CSR curve are indicative of a more regular, uniform pattern. The two statistical functions and their respective CSR conditions are further discussed in the Appendix.

RESULTS AND DISCUSSION

Stage 1: VES-FRCs Development

The Stage 1 results are presented in two sections: VES concretes without fibers, and VES-FRC mixtures with PP and S fibers.

VES Concretes Without Fibers

The laboratory batches of VES concretes without fibers were made at different fresh concrete and curing temperatures. Table 4 shows the fresh concrete properties for the batches of VES w/ SF and VES w/ FA. The air content values were within the VDOT specifications for all mixtures (VDOT, 2016). The slump values for the VES w/ FA were on the lower side because of the high heat generation.

Figure 9 shows the concrete temperature developments over the first 24 hours for the three VES w/ SF batches at three temperatures. The mixtures reached 3,000 psi compressive strength in over 13 hours, 8 hours, and 7 hours (indicated by black, solid circles in Figure 9) for mixtures with fresh concrete temperatures of 72 °F, 84 °F, and 90 °F, respectively. The results of tests conducted in accordance with the ASTM C918 and ASTM C1074 maturity methods using the Nurse-Saul function indicated the time the mixture with a fresh concrete temperature of 72 °F reached the required strength. The time of set varied for mixtures depending on the temperature. The time of set was about 5 hours, 4 hours, and 3 hours (indicated by red, dashed circles in Figure 9) for 72°F, 84 °F, and 90 °F mixtures, respectively. The temperature rise after the set was greater for the mixtures with higher initial fresh concrete temperatures, which indicates faster strength development.

Table 4. Fresh VES Concrete Properties

Property	VES w/ SF			VES w/ FA	
Air Content (%)	5	6	6	6	6
Unit Weight (lb/ft^3)	148	148	148	148	147
Slump (in)	6.8	3.5	3.5	3.5	4.5
Mix Temperature (°F)	72	84	90	75	85

Table 5 shows the compressive strength results for the VES w/ SF and VES w/ FA batches. The VES w/ FA mixtures reached 2,000 psi compressive strength within 7 hours. Therefore, it was expected that these mixtures would attain the desired 3,000 psi compressive strength within 10 hours based on maturity predictions.

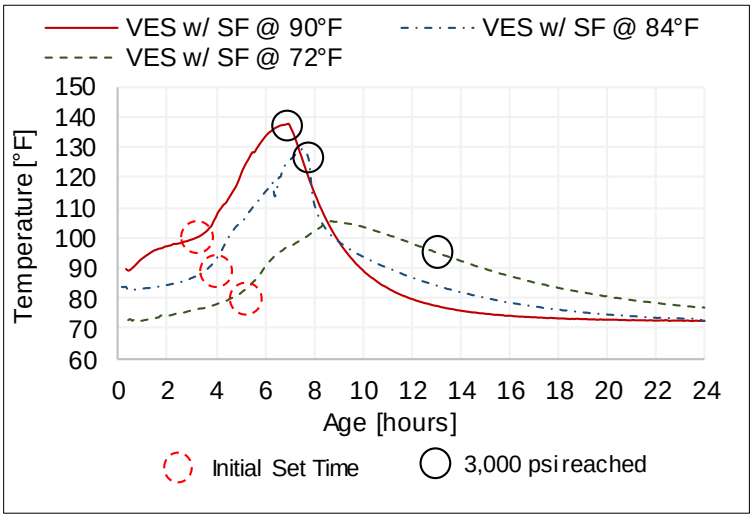

Figure 9. VES w/ SF Temperature Developments

Table 5. VES Concretes Compressive Strength Results

Age	VES w/ SF			VES w/ FA	
	72 °F	84 °F	90 °F	75 °F	85 °F
5 hours	-	-	830	-	-
6 hours	510	1,240	2,220	1,540	1,960
7 hours	1,180	2,330	3,190	2,810	2,360
8 hours	1,800	3,510	-	-	-
Maturity Prediction (13 hours)	3,000	-	-	-	-
24 hours	5,280	5,960	5,940	6,490	5,880
7 days	7,680	8,340	8,000	8,430	7,190
28 days	9,030	9,780	9,350	9,530	8,750

VES Concretes With Polypropylene or Steel Fibers

PP fibers and S fibers were added to the optimal VES w/ FA and VES w/ SF plain concrete mixtures. The amount of hardening accelerating admixture from batching was reduced from 30 oz/cwt to 20 oz/cwt to save on the total mixture cost. Hence, some acceptable reduction of the early age strength was expected.

The fresh concrete properties are presented in Table 6. Higher fresh concrete mix temperatures of 85 °F to 95 °F on average were used. The air contents of 5.7% on average were within VDOT specifications (VDOT, 2016). Because of high heat generation, the slump values were low, ranging from 2 to 5 in. The mixtures with PP had lower slump values compared to the mixtures with S, which was attributed to a lower dosage of high-range water-reducing admixture, the type of fiber, and a lower w/cm. However, the mixtures were still workable enough to be

placed in the molds. The molds were then capped to prevent evaporation. The shrinkage specimens during drying were kept in a special room with the relative humidity set to 50% ± 4% as required by ASTM C157.

The temperature developments of the four batches, i.e., VES-FRC w/ SF and PP or S fibers and VES-FRC w/ FA and PP or S fibers, are shown in Figure 10. The figure shows that the set time and strength gain of the VES-FRC w/ SF mixtures was about 1 hour slower than that of the VES-FRC w/ FA mixtures because of the difference in initial fresh concrete temperatures.

The temperature data confirmed the results of the compressive strength testing (Table 7). The VES-FRC w/ SF specimens reached 3,000 psi compressive strength within 8 to 8.5 hours, and the VES-FRC w/ FA specimens reached 3,000 psi within 7.5 to 8 hours. Flexural load-deflection plots of the laboratory VES-FRCs mixtures are presented in Figure 11. The increase in first-peak and residual flexural strengths with age is shown (Table 7).

Table 6. VES-FRCs Fresh Concrete Properties

Property	VES-FRC w/ SF		VES-FRC w/ FA	
	w/ PP Fibers	w/ S Fibers	w/ PP Fibers	w/ S Fibers
Air Content (%)	5.5	5.9	5	6.4
Unit Weight (lb/ft^3)	145	148	148	149
Slump (in)	4	5	2	3
Mix Temperature (°F)	85	90	97	94
Air Temperature (°F)	75	75	75	75

PP = polypropylene; S = steel.

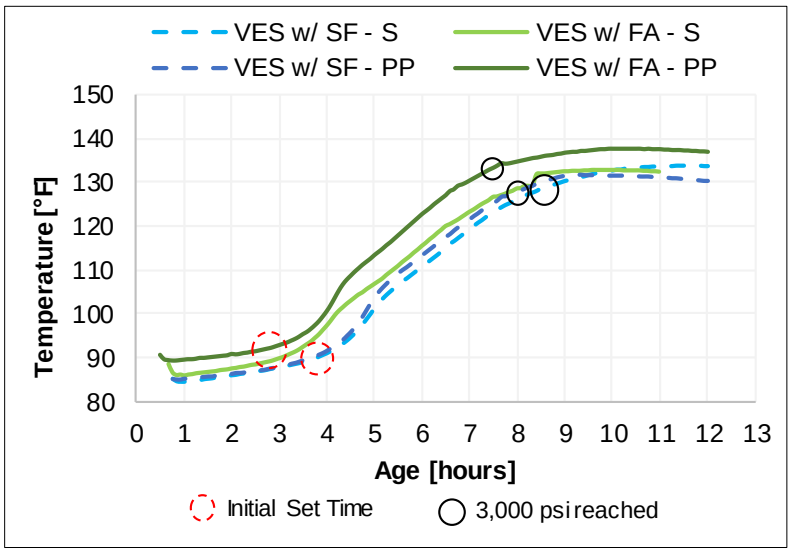

Figure 10. VES-FRCs Temperature Developments. PP = polypropylene fibers; S = steel fibers.

Table 7. VES-FRCs Hardened Properties

Test	Age	VES-FRC w/ SF		VES-FRC w/ FA	
		w/ PP	w/ S	w/ PP	w/ S
Compressive Strength (psi)	6.5 hours	1,890	950	2,930	2,540
	7.5 hours	2,530	2,780	3,860	2,840
	8 hours	-	-	-	3,160
	8.5 hours	4,150	3,220	-	-
	24 hours	6,700	7,540	5,240	4,380
	7 days	7,730	7,880	7,260	5,690
	28 days	8,780	8,880	8,860	8,890
First-Peak / Peak Flexural Strength (psi)	7.5-8.5 hours	490	460 / 620	375	465 / 475
	24 hours	690	715/ 1,030	660	665 / 1,135
	7 days	985	1,000	985	1,010 / 1,090
	28 days	1,075	1,100 / 1,380	1,095	1,115 / 1,290
Elastic Modulus (10^6 psi)	28 days	4.82	5.17	4.13	3.92

PP = polypropylene fibers; S = steel fibers; - = data not available.

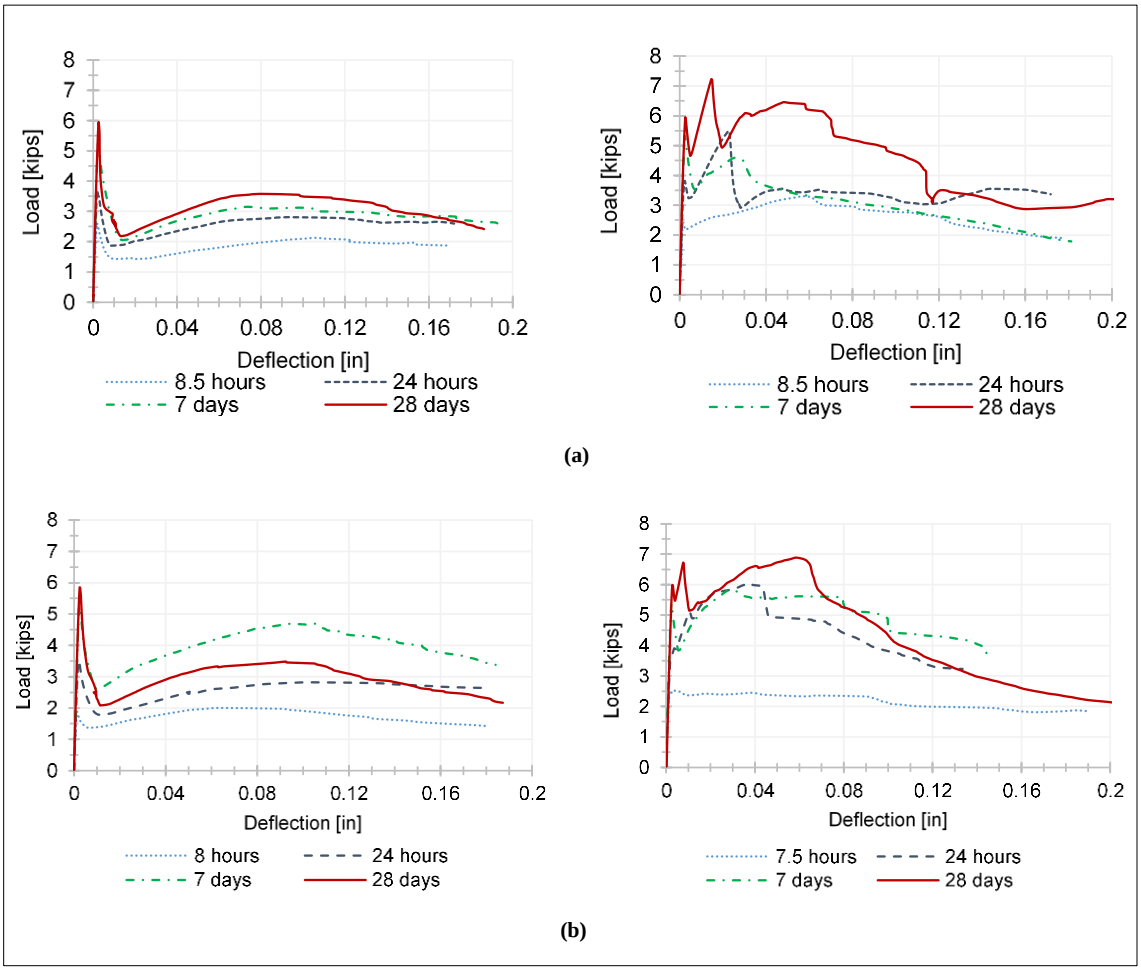

Figure 11. VES-FRCs with PP (left) and S (right) fibers for mixtures with (a) SF and (b) FA. PP = polypropylene fibers; S = steel fibers.

The first flexural specimens were tested at the time 3,000 psi compressive strength was reached. The VES-FRCs w/ SF beams were tested at 8.5 hours and reached a first-peak flexural strength of 490 and 460 psi for PP and S fiber specimens, respectively. The VES-FRC w/ FA beam specimens were tested at 7.5 and 8 hours, resulting in first-peak flexural strength of 375 and 465 psi for PP and S fiber specimens, respectively. These values exceeded the flexural strength requirement of 350 psi from the study on VES concretes previously discussed (Punurai et al., 2007). Further, the flexural strength values met the strength requirements of 260 to 400 psi reported in the study by Van Dam et al. (2005) for the 6- to 8-hour concrete repair materials.

For both VES-FRC w/ SF and VES-FRC w/ FA, the mixtures with S fibers had better post-cracking performance than the mixtures with PP fibers, with better deflection hardening behavior and higher residual strength and toughness values. Toughness at L/150 deflection value was almost double for the specimens with S fibers compared to the samples with PP fibers (Table 8). Similar trends can be observed for the residual strength and equivalent flexural strength ratio values, which indicate the ratio of residual strength to the first-peak strength. The flexural capacity of the VES-FRCs with S fibers was 93% on average after the first-peak crack, and the capacity of the VES-FRCs with PP fibers was about 49% on average.

Figure 12 shows the drying shrinkage values for both VES-FRC types. At 4 months, both VES-FRC w/ FA and VES-FRC w/ SF had length change values up to 0.07% on average, which is at the suggested limit of 0.07% at 4 months. However, the shrinkage values at 28 days were greater than the recommended value of 0.040% (Babaei and Fouladgar, 1997). VDOT uses a maximum value of 0.035% at 28 days for low cracking bridge decks (VDOT, 2016). In addition, the paste contents of 0.32 and 0.33 for VES-FRCs w/ SF and w/ FA, respectively, exceeded the recommended 0.27 paste content limit (Darwin et al., 2004). High cement contents of 750 lb/yd^3 and high paste contents for both batches detrimentally affected the shrinkage performance of the concretes, making them prone to cracking.

Table 8. Laboratory VES-FRCs 28-Day Flexural Results

Test	VES-FRC w/ SF		VES-FRC w/ FA	
	w/ PP	w/ S	w/ PP	w/ S
First-Peak / Peak Flexural Strength (psi)	1075	1100 / 1380	1095	1115 / 1290
Toughness, (in-lb)	230	450	220	430
Residual Strength (psi)	430 / 640	1160 / 860	405 / 570	1040 / 910
Equivalent Flexural Strength Ratio (%)	51	96	46	90

PP = polypropylene fibers; S = steel fibers.

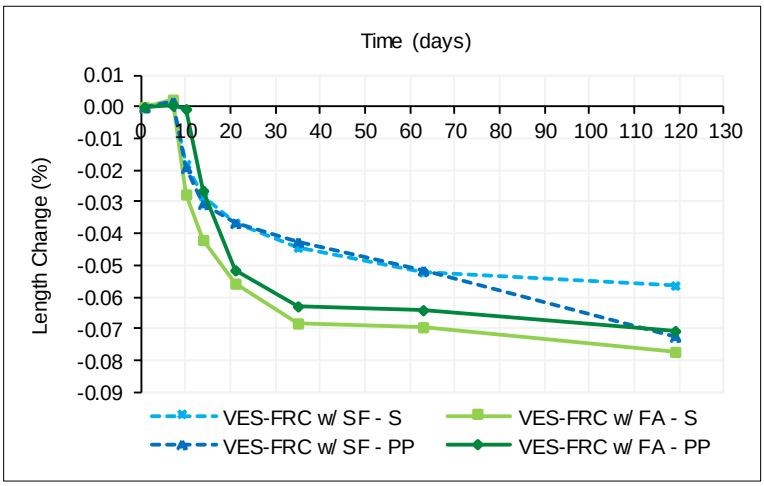

Figure 12. VES-FRC Drying Shrinkage Results

Stage 2: Permeability of Cracked FRC Specimens

The second stage of the study focused on water permeability testing of the cracked FRC specimens. A total of 66 samples were analyzed. The crack widths of 0.1 to 0.5 mm (0.004 to 0.020 in) under load were formed in accordance with the ASTM C496 splitting tensile testing procedure. Figure 13 displays the crack width recovery after unloading. The solid black line represents theoretical no recovery values. The VES-FRCs followed the same trend of recovery, and on average all specimens recovered more than 43% of the crack width.

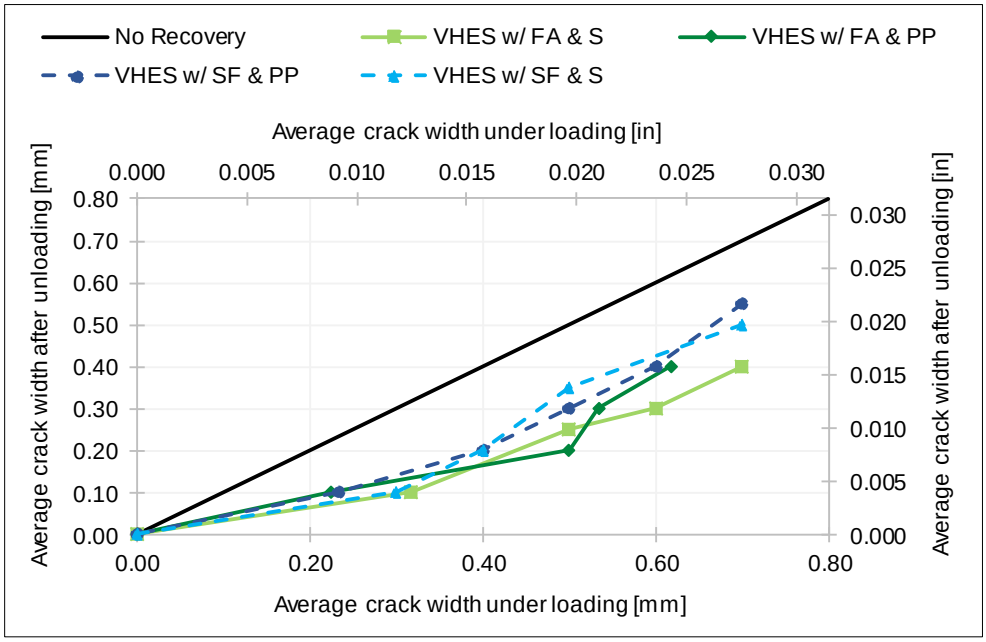

Figure 13. Average Crack Width Recovery for VES-FRCs. S = steel fibers; PP = polypropylene fibers.

During the splitting tensile test, the crack would start forming in the center of the cross section of the specimen, extending to the edges with further load applied. Figure 14 displays an example specimen with the formed crack and unloaded crack widths for various specimens measured with the magnifier.

The crack widths were measured at the top, middle, and bottom section on both sides of the specimen, and the crack width that was observed the most was used as a final crack width of that specimen. The correlation between the laser system and magnifier with a scale revealed a difference of just a little more than 10% on average. This difference was deemed to be acceptable because of the irregularity of the crack width and crack patterns.

The CWP was calculated using Equation 1. Figure 15 shows the VES-FRCs permeability results. The CWP values approximately follow the same trend for all concretes, and the observed variation could be due to the irregularity of crack size and pattern. This means that the crack width was the controlling factor, not the FRC material or fiber type. An increase in the CWPs for increased crack widths can be observed. For VES-FRC specimens, the increase in the CWP by 20 times on average was observed for crack widths increasing from 0.1 to 0.2 mm. The specimen of VES-FRC w/ FA and PP fibers had an increase of more than 300 times.

Typical values of the CWP for normal strength and high strength concretes were about 10^{-10} cm/s and less than 10^{-14} cm/s, respectively (Nawy, 2001). The solid VES-FRC specimens had CWP values on the order of 10^{-10} cm/s, consistent with the lower water permeability limits reported by Wang et al. (1997). The CWP values were above 10^{-6} to 10^{-5} cm/s for specimens with crack widths greater than 0.1 mm and above 10^{-3} cm/s for cracks greater than 0.2 mm. In this case, the corrosion of primary reinforcement because of leakage through cracks with widths greater than 0.1 mm is highly probable.

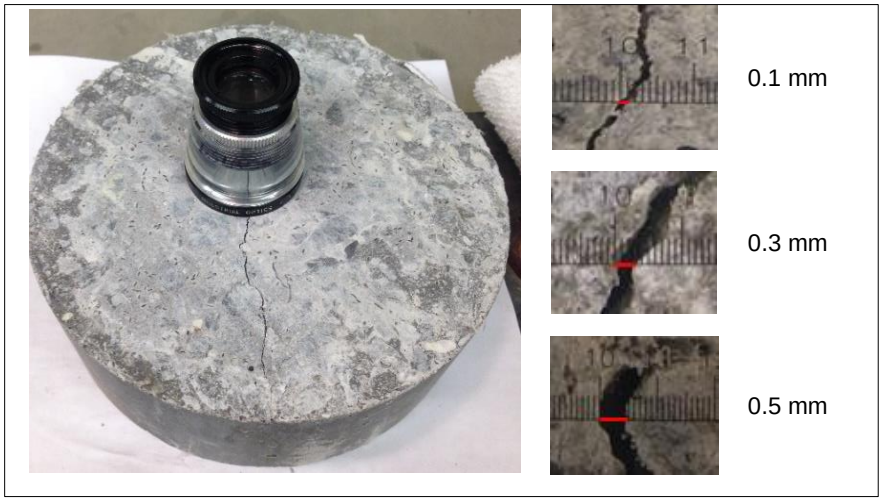

Figure 14. Example Specimens: Formed Crack and Unloaded Crack Widths

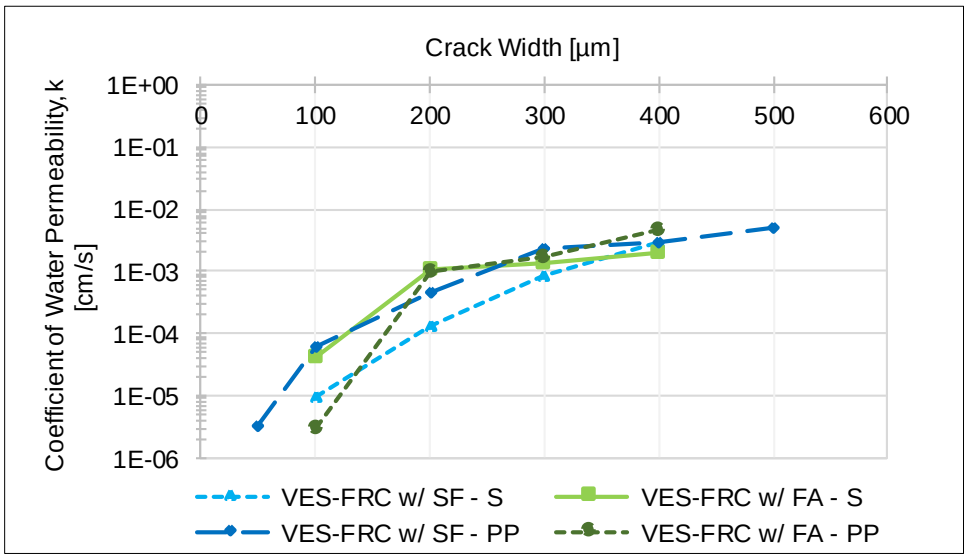

Figure 15. Coefficient of Water Permeability Versus Crack Width. Conversion factors: 100 µm = 0.1 mm = 0.0039 in. S = steel fibers. PP = polypropylene fibers.

In addition, the results were compared with those in the literature. The threshold of 0.05 to 0.10 mm crack widths was not available in this study. There was a difference in CWP compared to this study that was mainly attributed to the difficulty of obtaining uniform cracks in the specimens. However, the data comparison among different studies showed similar trends but did not have an adequate correlation. The crack formation process and highly irregular crack widths were most likely the cause. Cracks less than 0.1 mm in width were difficult to form with the rate of loading applied. In the future, slower loading rates are recommended to form tighter cracks.

Stage 3: Fiber Distribution Analysis

This stage of the study focused on the analysis of fiber distribution. Fiber density and spatial fiber dispersion were examined. Two cutting methods were used: HTH and THTHT. Figure 16 shows a more complete fiber distribution analysis.

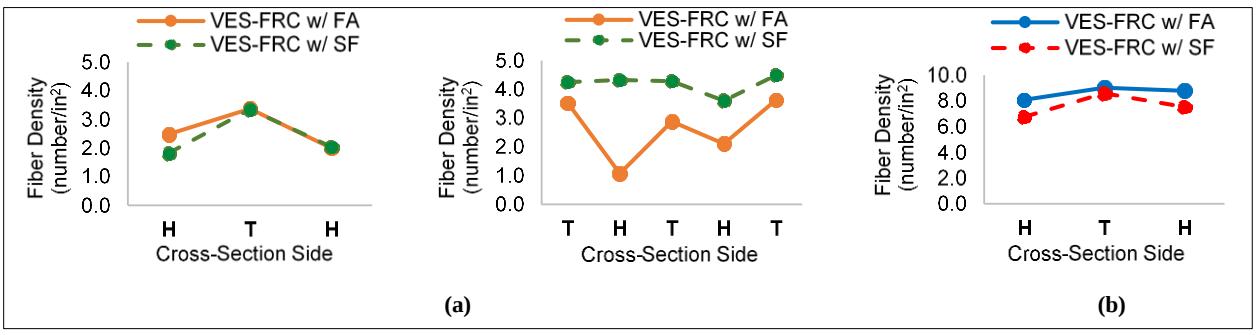

Figure 16. Fiber Density per Cross-Section Side for HTH and THTHT: (a) Steel fibers; (b) Polypropylene fibers. H = horizontal cut; T = transverse cut.

Figure 16 shows the average fiber density for T and H cross sections for S fibers and PP fibers. As may be seen, the S fibers had a tendency to align parallel along the length of the beam in a T direction. This alignment is beneficial to the flexural and tensile capacities of the specimens because of the greater number of fibers at the beam crack face effectively resisting the applied normal stresses. The fiber preferential alignment could be due to the beam size and casting methods. For the PP fiber samples, the alignment in the T direction is less pronounced compared to the S fiber samples (Figure 16b). In this case, the fibers were more evenly aligned and equally distributed in both the T and H directions. This could be due to the smaller fiber length of 2 in and the flexibility of the synthetic fibers.

In addition, statistical spatial point pattern analysis was performed to examine the fiber distribution on both sides of the crack (see Figure 17). The calculated $(K[s] / \pi)^{1/2}$ function and F-function average values were compared to the theoretical CSR values, K-CSR and F-CSR, respectively. For the S fiber specimens, the VES-FRC w/ SF samples had more fiber clumping compared to the samples with FA.

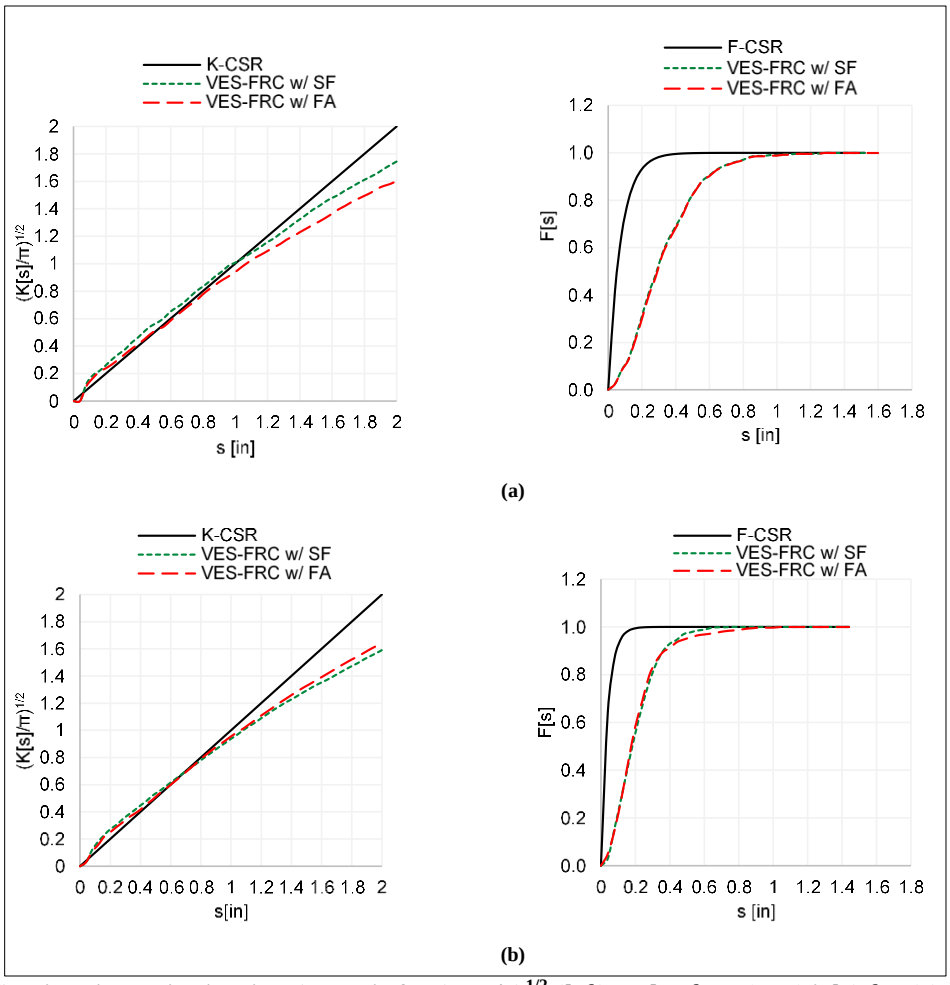

Figure 17. Spatial Fiber Distribution Analysis for $(K[s]/\pi)^{1/2}$ (*left*) and F-function (*right*) for (a) Steel Fibers and (b) Polypropylene Fibers

The VES-FRC w/ FA had values closer to the K-CSR curve, indicating more of a random distribution (Figure 17a). The VES-FRCs with PP fibers displayed similar spatial fiber dispersion for both SF and FA mixtures, displaying some degree of fiber clumping (Figure 17b). From the F-function results, it is apparent that all samples displayed a certain level of fiber clumping and a number of empty areas without fibers, with the slopes less steep than those of the F-CSR curves.

CONCLUSIONS

- *VES-FRCs with different fiber types and dosages and silica fume or fly ash can provide durable concretes and facilitate rapid construction.*

- *A compressive strength of 3,000 psi within 10 hours can be achieved with the use of increased amounts of cement, low w/cms, increased fresh concrete temperatures above 80 °F, accelerating admixtures, and insulated curing.*

- *High residual strengths and resistance to cracking can be achieved with the addition of fibers.* VES-FRCs with S fibers had superior post-cracking performance compared to VES-FRCs with PP fibers.

- *VES-FRCs had high paste contents and high shrinkage values, making them prone to cracking.* However, the addition of fibers is expected to facilitate crack control through residual flexural strength and toughness.

- *Water permeability increases with increases in crack width.* The CWP values for solid VES-FRC specimens were consistent with the lower water permeability limits reported in the literature. Cracks wider than 0.1 mm allow for intrusion of harmful solutions. Cracking control can be achieved through fiber addition.

- *S fibers in specimens demonstrate preferential alignment.* The fiber distribution analysis demonstrated that the S fibers had a tendency to align parallel along the length of the beam, which is beneficial to the flexural and tensile capacities of the specimens. The PP fibers were more equally distributed in all directions. The statistical analysis of spatial fiber patterns showed that all FRC systems had a tendency for fiber clumping to various degrees.

RECOMMENDATIONS

- This was a preliminary study investigating the feasibility of using very early strength and durable fiber-reinforced concretes. Therefore, there is no recommendation for implementation at this time.

BENEFITS AND IMPLEMENTATION

Benefits

Because of the deteriorating state of the existing transportation infrastructure, there is a need for high-performance repair materials. The VES-FRC mixtures developed in this study provide early strength for faster repairs and exhibit enhanced durability for improved performance. The early strength property of the mixtures will help with minimizing traffic interruptions and user costs; the controlled cracking and low-permeability characteristics are expected to contribute to the extension of the service life of structures, thus reducing maintenance repairs.

Implementation

Additional research is needed to develop mixtures that can be implemented by VDOT. A project should be initiated in which VES-FRC mixtures should be optimized further for strength and durability through evaluation of ingredients and mixture proportions designed for application of traffic at different ages. Promising mixtures should be tried in the field. Field applications should address different projects where quantities of concrete vary from small batches measured in cubic feet to larger mixtures in cubic yards. Therefore, for field concretes, mixing in ready-mixed concrete trucks, mobile mixers, and mortar mixers and even mixing in small buckets should be investigated to address the size of the project.

The approval of these concretes can be prescriptive or performance based including different tolerances. Work in the laboratory and the field along with consultation with experts is expected to lead to a recommendation that would include a specification. The specification should be prepared by VTRC and VDOT's Materials Division to enable the implementation of VES-FRCs in VDOT applications.

ACKNOWLEDGMENTS

The authors thank VTRC research and technical staff for their assistance and guidance in this study, specifically Michael Burton, James Copeland, Troy Deeds, Kenneth Herrick, Stephen Lane, Andrew Mills, William Ordel, Keith Peres, and Xuemeng "John" Xia. Further, the authors thank the industry for their input and assistance with this study. The authors thank the University of Virginia, specifically Devin Harris, for providing guidance throughout this study; personnel of VDOT's Materials Division and Structure and Bridge Division and VDOT's Staunton District; and the Federal Highway Administration. The authors also thank the technical review panel, William Bailey, Lance Dougald, Larry Lundy, Harikrishnan Nair, Prasad Nallapaneni, and Rex Pearce; former VTRC Director Jose Gomez; VTRC Associate Director Michael Sprinkel; and the editor Linda Evans.

REFERENCES

American Concrete Institute. *Control of Cracking in Concrete Structures.* ACI 244R-01. Farmington Hills, MI, 2001.

American Concrete Institute. *Report on Fiber Reinforced Concrete.* ACI 544.1R-96. Farmington Hills, MI, 2009.

American Concrete Institute. *Report on High-Strength Concrete.* ACI 363R-10. Farmington Hills, MI, 2015.

Akkaya, Y., Peled, A., and Shah, S.P. Parameters Related to Fiber Length and Processing in Cementitious Composites. *Materials and Structures,* Vol. 33, No. 8, 2000a, pp. 515-524.

Akkaya, Y., Picka, J., and Shah, S.P. Spatial Distribution of Aligned Short Fibers in Cement Composites. *Journal of Materials in Civil Engineering,* Vol. 12, No. 3, 2000b, pp. 272-279.

Akkaya, Y., Shah, S.P., and Ankenman, B. Effect of Fiber Dispersion on Multiple Cracking of Cement Composites. *Journal of Engineering Mechanics,* Vol. 127, No. 4, 2011, pp. 11-316.

Aldea, C.-M., Shah, S.P., and Karr, A. Permeability of Cracked Concrete. *Materials and Structures,* Vol. 32, No. 5, 1999, pp. 370-376.

ASTM International. *ASTM Standard C1609/C1609M-12: Flexural Performance of Fiber-Reinforced Concrete (Using Beam With Third-Point Loading).* West Conshohocken, PA, 2013.

Babaei, K., and Fouladgar, A.M. Solutions to Concrete Bridge Deck Cracking. *Concrete International,* Vol. 19, No. 7, 1997, pp. 34-37.

Darwin, D., Browning, J., and Lindquist, W.D. Control of Cracking in Bridge Decks: Observations From the Field. *Cement, Concrete, and Aggregates,* Vol. 26, No. 2, 2004, pp. 148-154.

Diggle, P.J. *Statistical Analysis of Spatial Point Patterns.* Hodder Education Publishers, London, 2003.

Granju, J.-L., and Balouch, S.U. Corrosion of Steel Fibre Reinforced Concrete From the Cracks. *Cement and Concrete Research,* Vol. 35, No. 3, 2005, pp. 572–577.

Kang, S.T., and Kim, J.K. The Relation Between Fiber Orientation and Tensile Behavior in an Ultra-High Performance Fiber Reinforced Cementitious Composite (UHPFRCC). *Cement and Concrete Research,* Vol. 41, No. 10, 2011, pp. 1001-1014.

Kang, S.T., and Kim, J.K. Investigation on the Flexural Behavior of UHPCC Considering the Effect of Fiber Orientation Distribution. *Construction and Building Materials,* Vol. 28, No. 1, 2012, pp. 57-65.

Kang, S.T., Lee, B.Y., Kim, J.-K., and Kim, Y.Y. The Effect of Fibre Distribution Characteristics on the Flexural Strength of Steel Fibre-Reinforced Ultra-High Strength Concrete. *Construction and Building Materials,* Vol. 25, No. 5, 2011, pp. 2450-2457.

Klieger, P. Effect of Mixing and Curing Temperature on Concrete Strength. *Journal of the American Concrete Institute,* Vol. 54, No. 62, 1958, pp. 1063-1081.

Kosmatka, S.H., and Wilson, M.L. *Design and Control of Concrete Mixtures.* Portland Cement Association, Skokie, IL, 2011.

Mangat, P.S., and Gurusamy K. Permissible Crack Widths in Steel Fibre Reinforced Marine Concrete. *Materials and Structures,* Vol. 20, No. 5, 1987, pp. 338–347.

Mehta, P.K., and Burrows, R.W. Building Durable Structures in the 21st Century. *Concrete International,* Vol. 23, No. 3, 2011, pp. 57-63.

National Bridge Inventory. *Highway Bridges by Superstructure Material 2015.* Federal Highway Administration, Washington, DC, 2015.

Nawy, E.G. *Fundamentals of High-Performance Concrete.* John Wiley & Sons, New York, 2001.

Ozyildirim, C. High-Performance Concrete for Transportation Structures. *Concrete International,* Vol. 15, No. 1, 1993, pp. 33-38.

Ozyildirim, C., Moen, C., and Hladky, S. *Investigation of Fiber-Reinforced Concrete for Use in Transportation Structures.* VTRC 97-R15. Virginia Transportation Research Council, Charlottesville, 1997.

Parker, F., and Shoemaker, W.L. PCC Pavement Patching Materials and Procedures. *Journal of Materials in Civil Engineering,* Vol. 3, No. 1, 1991, pp. 29-47.

Portland Cement Association. *Fiber Reinforced Concrete.* Skokie, IL, 1991.

Punurai, S., Punurai, W., and Hsu, C.-T.T. A Very Early Strength Concrete for Highway Construction. *Journal of Testing and Evaluation,* Vol. 35, No. 6, 2007, pp. 1-9.

Rapoport, J., Aldea, C.-M., Shah, S.P., Bruce, A., and Karr, A. *Permeability of Cracked Steel Fiber-Reinforced Concrete.* National Institute of Statistical Sciences, Durham, NC, 2001.

Shah, S.P., and Wang, K. Microstructure, Microcracking, Permeability, and Mix Design Criteria of Concrete. *Fifth International Conference on Structural Failure, Durability and Retrofitting,* Singapore, 1997, pp. 260-272.

Sprinkel, M.M. Research Pays Off: Very Early Strength Latex-Modified Concrete Bridge Overlays: Virginia's Quick Cure for Roadway Maintenance Delays. *TR News*, Vol. 247, December, 2006, pp. 34-35.

Van Dam, T.J., Peterson, K.R., Sutter, L.L., Panguluri, A., Sytsma, J. Buch, N., Kowli, R. and Desaraju, P. *Guidelines for Early-Opening to Traffic Portland Cement Concrete for Pavement Rehabilitation.* NCHRP Report 540. Transportation Research Board of the National Academies, Washington, DC, 2005.

Vanikar, S.N., and Triandafilou, L.N. *Implementation of High-Performance Concrete Bridge Technology in the USA.* ACI SP-228. Seventh International Symposium on the Utilization of High-Strength /High-Performance Concrete, Washington, D.C., 2005, pp. 1-12.

Virginia Department of Transportation. *Virginia Test Method 120: Method of Test for Measurement of Permeability of Bituminous Paving Mixtures Using a Flexible Wall Permeameter—(Asphalt Lab).* Richmond, 2005.

Virginia Department of Transportation. *State of the Structures and Bridges Report.* Richmond, 2015.

Virginia Department of Transportation. *Road and Bridge Specifications.* Richmond, 2016.

Wang, K., Jansen, D.C., Shah, S.P., and Karr, A.F. Permeability Study of Cracked Concrete. *Cement and Concrete Research*, Vol. 27, No. 3, 1997, pp. 381-393.

APPENDIX

STATISTICAL SPATIAL K-FUNCTION AND F-FUNCTION

The methods used to determine the two statistical point pattern functions are explained graphically in Figure A1. The K-function considers a number of fibers within distance **s** of an arbitrary fiber in the cross-section. Distance *s* was varied from 0 to one-half the width of the specimen. The F-function can be used to measure the empty spaces between the fibers. It determines the distribution of distances *s* from a random sample point in the cross-section or from a generated grid point to its nearest fiber. For the F-function, the grid point method was used. Diggle (2003) recommended using a $k \times k$ grid to represent the sample points, where

$$k \approx \sqrt{number\ of\ fibers}.$$

The grid dimensions were twice the *k* value. The size of *k* does not improve the statistical precision but facilitates the smoothness of the curve.

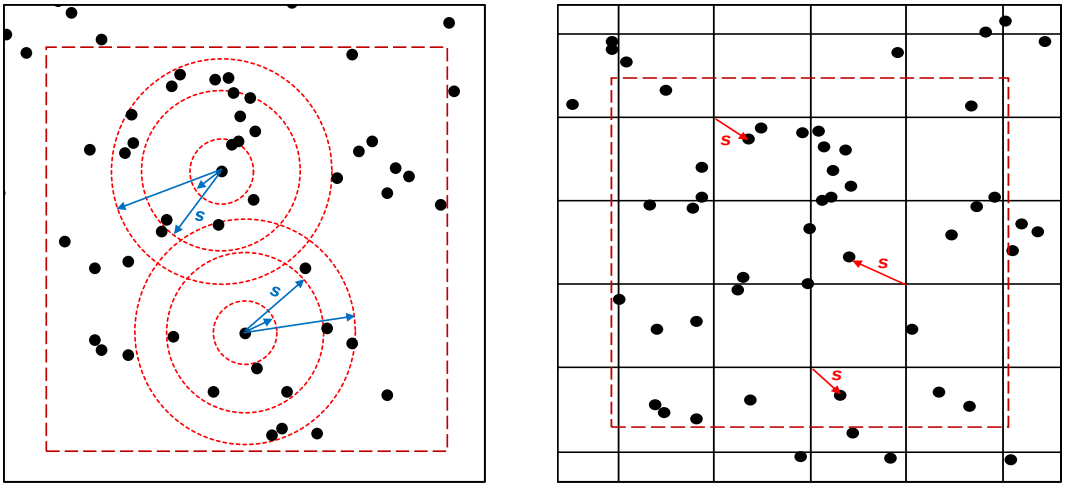

Figure A1. Methods Used to Determine the Two Statistical Point Pattern Functions: (a) K-function; (b) F-function. Adapted from Akkaya et al., 2000b.

The K-function is calculated by using Equation A1:

$$K(s) = \frac{Number\ of\ fibers\ within\ distance\ \boldsymbol{s}\ of\ an\ arbitraty\ fiber}{(Total\ number\ of\ such\ fibers) \cdot \lambda} \qquad \text{[Eq. A1]}$$

where λ is a fiber density and is represented by Equation A2:

$$\lambda = \frac{Expected\ number\ of\ fibers}{Unit\ Study\ Area} \qquad \text{[Eq. A2]}$$

The F-function can be calculated by using Equation A3:

$$F(s) = \frac{Number\ of\ sample\ points\ in\ the\ study\ area\ with\ nearest\ fiber\ within\ distance\ \boldsymbol{s}}{Total\ number\ of\ sample\ points\ in\ the\ study\ area} \quad \text{[Eq. A3]}$$

Under a CSR condition for a homogeneous Poisson process, the K-function and F-function are calculated using Equation A4 and Equation A5, respectively.

$$K(s) = \pi s^2 \quad \text{[Eq. A4]}$$

$$F(s) = 1 - e^{(-\lambda \pi s^2)} \quad \text{[Eq. A5]}$$

Graphic representations of

$$\left(\frac{K[s]}{\pi}\right)^{\frac{1}{2}}$$

and F-function curves for clustered, regular, and random point pattern distributions are represented in Figure A2. The value of $(K[s]/\pi)^{1/2}$ equals the distance *s* (see Equation A4 for reference).

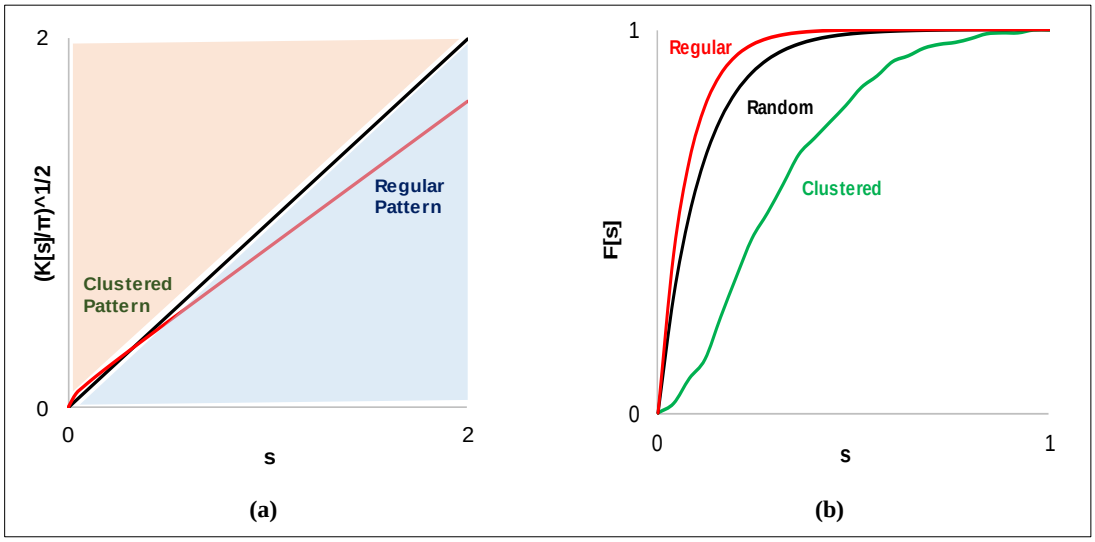

Figure A2. Graphic Representations of (a) $(K[s]/\pi)^{1/2}$ Function, and (b) F-function

In addition, the edge effects were considered through a buffer zone (red dotted box in Figure A1). A study area of observation inside the beam cross-section area a certain distance away from the edges was selected to account for edge effects. The calculated values are more precise for the smaller *s* distances because they are less likely to be affected by the edge effects.